Improved implementation and application of the individually selecting configuration interaction method

P. Stampfuß and W. Wenzel

Forschungszentrum Karlsruhe, Institut für Nanotechnologie, Postfach 3640, 76021 Karlsruhe, Germany

We report on the progress of our implementation of the configuration-selecting multireference configuration interaction method on massively parallel architectures with distributed memory, which now permits the treatment of Hilbert spaces of dimension $O(10^{12})$. Of these about 50 000 000 can be selected in the variational subspace. We provide scaling data for the running time of the code for the IBM/SP3 and the CRAY-T3E. We present benchmark results for two selected applications: the energetics of the isomers of dinitrosoethylene and the benchmark results for the ring closure reaction of enediyene.

I. INTRODUCTION

The multireference configuration interaction method (MRCI) is one of the established benchmark methods that offer a systematic approach for the calculation of the electronic structure of atoms and molecules.[1–3] An accurate quantum chemical treatment of complex molecules requires a balanced account of both dynamical and nondynamical correlation effects. The latter are particularly important when one wants to describe an entire potential energy surface, where bond breaking or bond rearrangements can occur. To adequately describe these effects, as well as for the treatment of electronically excited states, a wave function based method must accommodate the multireference nature of the electronic states. Dynamical correlation effects, i.e., the mutual influence electrons exercise on each other when they pass at close distance, are incorporated by considering excitations of the set of relevant reference configurations. The generic lack of extensivity of MRCI methods has at least been partially addressed with a number of *a posteriori*[4,5] corrections and through direct modification of the CI energy functional.[6–10]

Due to its high computational cost applications of the MRCI method remain constrained to relatively small systems. For this reason the configuration-selective MRCI method (MRD-CI),[11–13] has become one of its most widely used versions. In this variant only the most important configurations of the interacting space of a given set of primary configurations are chosen for the variational wave function, while the energy contributions of the remaining configurations are estimated on the basis of second-order Rayleigh–Schrödinger perturbation theory.[14,15] Even within this approximation, the cost of MRCI calculations remains rather high. The development of efficient configuration-selecting CI codes[15–22] is inherently complicated by the sparseness and the lack of structure of the selected state vector. In order to extend the applicability of the method, it is desirable to employ the most powerful computational architectures available for such calculations.

Here we report improvements of our massively parallel, residue-driven implementation of the MRD-CI method for distributed memory architectures.[22] In this implementation the difficulty of the construction of the subset of nonzero matrix elements is overcome by the use of a residue-based representation of the matrix elements that was originally developed for the distributed memory implementation of MR-SDCI.[21] This approach allows to efficiently evaluate the matrix elements both in the expansion loop as well as during the variational improvement of the coefficients of the selected vectors.

This manuscript is organized as follows: In Sec. I we report recent improvements of the massively parallel MRD-CI implementation that permit the treatment of larger Hilbert spaces, i.e., the correlation of a larger number of electrons in larger basis sets. We demonstrate the scalability of the integral driven version of the matrix element evaluation routine on two widely available massively parallel architectures, the CRAY-T3E and the IBM-SP3/SMP. We then elucidate applicability and limitations of MRD-CI in benchmark applications for two sensitive chemical problems: the ring-closure reaction of enediyeneand the electronic structure of benzofuroxan/dinitrosoethylene.

II. TECHNICAL IMPROVEMENTS

In the transition residue driven approach each matrix element between two determinants (or configuration state functions $|\phi_1\rangle$ and $|\phi_2\rangle$) is associated with the subset of orbitals that occur in both the target and the source determinants.[21,22] This unique subset of orbitals called the *transition residue* is mediating the matrix element and serves as a sorting criterion to facilitate the matrix element evaluation on distributed memory architectures. For a given many-body state, we consider a tree of all possible transition residues as illustrated in Fig. 1. For each such residue we build a list of *residue entries*, composed of the orbital pairs (or orbital for a single-particle residue), which combine with the residue to yield a selected configuration and a pointer to that configuration. While the number of transition residues is comparatively small, the overall number of residue entries grows rapidly (as $N_{\text{selected}} n_e^2$) with the number of configurations N_{selected} and the number of electrons n_e.

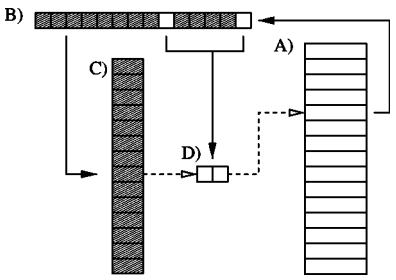

FIG. 1. Schematic representation of the residue tree: (a) list of globally indexed many-body configuration, (b) a specific many-body configuration with 14 electrons. Each possibility to remove two orbitals from the configuration (white boxes) generates an entry in the residue table (c) and an associated orbitals pair (d), which is stored together with the index of the original configurations. Solid arrows indicate the operations of building the residue tree dashed arrows the logical connection between its elements. The residue tree (c) is a list of transition residues. Associated with each residue is a list of entries, consisting of the orbital pairs and the index of the configuration that generated the entry.

Once the residue tree is available the evaluation of the matrix elements is very efficient. For each transition residue, each pair of entries of type D in Fig. 1 generates a matrix element. The indices of the right- and left-hand side configurations are stored in the entries and the indices of the orbital pair generate the matrix element. If all entries of the residue tree are generated, its size limits the number of configurations in the variational subspace. In order to increase the size of the variational subspace we have removed all transition residues containing two external orbitals from the residue tree, reducing the size of the residue tree by more than an order of magnitude. Matrix elements mediated by such transition residues can be computed by gathering all elements of the coefficient vector that contain a particular external pair on a single node of the machine. We have implemented a scheme that efficiently evaluates the orbital difference map of the internal part of two such configurations to determine if a nonzero matrix element exists. The value of the associated integral element is easily obtained from the (small) table of all integrals with only internal indices which we replicate on each node. Implementing this change reduces the size of the residue tree significantly and allows to increase the size of the variational subspace by almost a factor of 10, to about 20×10^6 configurations.

Improving the previous implementation,[23] we now split the state vectors for the Davidson iteration across all nodes, such that only two copies of the total state vector are required on each node for the evaluation of the matrix elements. For 50×10^6 configurations, a 64-bit representation of the state vector requires 400 MB storage per vector and remains the last large undistributed data element in our implementation. Even these can be eliminated, at the expense of locally increasing the residue tree. Instead of storing only the configuration index in the residue tree, one may also store the coefficient of the left- and right-hand side vectors of the matrix element, scattering the former and gather in the latter before and after the matrix element evaluation, respectively.

Requirements for the integral storage could also be drastically reduced by splitting the integral file sorted in physics notation across all nodes. Once the residue tree has been constructed, its ''heads,'' i.e., the information regarding the transition residue itself can be discarded. During the matrix evaluation, only the orbital lists are required. The space freed by eliminating the information pertaining to the content of the individual residues can be reused to address those orbital lists that contain a particular orbital pair. Once a set of integrals $\langle i_1 i_2 | i_3 i_4 \rangle$ with a given orbital pair, e.g., $i_1 i_2$, is served to the node, this information can be used to identify all orbital lists that generate nonzero matrix elements for this integral list. Using this information, an *integral driven* matrix element evaluation scheme can be implemented, during which all integral lists $\langle i_1 i_2 | \ldots \rangle$ are distributed across the nodes and rotated in a cyclic fashion until every integral list has visited every node. Since MPI permits a very fast cyclic data exchange and no search operations are required to identify nonzero matrix elements for a given set of integrals, this mechanism allows for efficient integral driven evaluation of all matrix elements not mediated by doubly external transition residues.

To demonstrate the performance of the improved code we have performed model calculations on two common massively parallel architectures with distributed memory, the CRAY T3E and the IBM-SP/SMP for a varying number of nodes. We report the total CPU (wall clock) time of each calculation and decompose it into several important, not necessarily contiguous portions, comprising (a) the generation of the integrals, self-consistent-field, four-index transforms; (b) the generation and distribution of the residue tree; (c) the iterative generation of approximate natural orbitals (NO) in BW-MRPT Ref. 24 (five iterations of the NO loop, which is very similar to the MRD-CI selection step); and (d) the subsequent selection and iteration of a single state in the selected Hilbert space (five iterations). In an ideal massively parallel implementation the total CPU time should be independent of the number of nodes (scalability) and competitive with a serial implementation (efficiency). The numerical cost of NO generation, expansion, and iteration is usually directly proportional to the number of roots in one symmetry. The ''logic'' cost of generating the residue tree is proportional to the number of configurations multiplied with the number of electrons squared. The numerical cost of the iteration step depends on the average of the square of the the number of orbital pairs per transition residue, multiplied with the number of transition residues. In a nonselecting MR-SDCI calculation, this number would again scale as the number of orbitals squared. If comparatively few configurations of the overall Hilbert space are selected, the residue tree can be relatively sparse. In this case the numerical effort creating the residue tree becomes comparable to the effort evaluating the matrix elements.

Figure 2 shows a scaling plot for a calculation selecting 3.7×10^6 of 2×10^7 configurations running on 32–256 nodes of the CRAY TE3 of the NIC Jülich, which demonstrates that the calculation scales well from 32–128 nodes, with a significant loss of efficiency in the last doubling of the number of processors to 256 nodes. The fourfold increase of the number of nodes from 32 to 128 leads to total loss of efficiency of about 24% for the total calculation or 18% for the MRD-CI calculation alone. This reflects the fact that we have

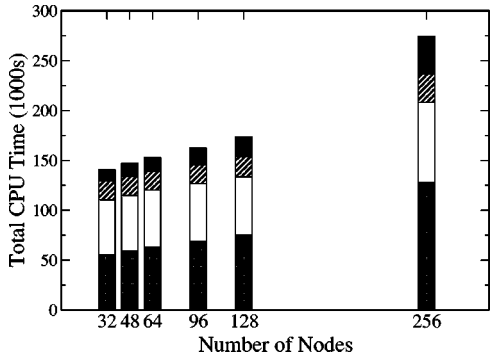

FIG. 2. Scaling plot of the total CPU time vs the number of nodes for a massively parallel MRD-CI calculation selecting 3.7×10^6 of 2×10^7 determinants running on 32–256 nodes on the CRAY-T3E. The individual contributions (from the top) are preparation (integral generation, SCF, four-index transform), logic (building and redistributing the residue tables) and configuration selection (including the perturbative calculation of the approximate natural orbitals in five iterations) and the iteration of the selected state-vector, respectively.

focused our efforts mostly on the performance of the MRD-CI code, rather than on the preceding calculations. Among the components of the MRD-CI, the iteration loop scales worst, with a total loss of 35% in its efficiency. This results from the fact that the load balancing of the matrix element evaluation in the integral driven mode becomes progressively difficult as the number of matrix elements is reduced. As the integrals are distributed cyclically in batches among the nodes, the entire calculation must wait for the slowest node to finish each integral batch. The size of the calculation was chosen to make runs on relatively few nodes possible. It is therefore not surprising that this calculation does not perform well on 256 nodes, where about 80% of the efficiency is lost. If the size of the selected space is increased, the performance loss between 128 and 256 nodes is reduced, but the calculation no longer runs on 32 nodes.

Figure 3 shows a scaling plot for a similar calculation for dinitrosoethylene (DNE) on an IBM SMP/SP3 with 64 processors. Quadrupling the number of processors here, results only in a marginal loss of 12% of the overall efficiency of the calculation, the iteration loop again scales worst (34% loss). The better performance of the IBM for this calculation is

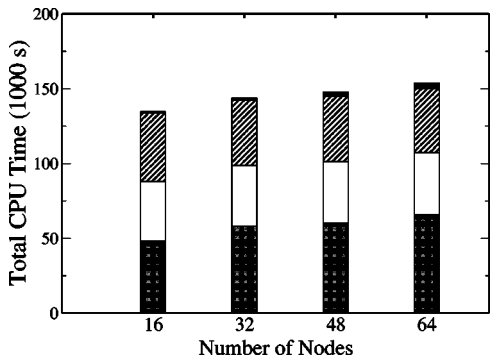

FIG. 3. Scaling plot of the total CPU time vs the number of nodes for a massively parallel MRD-CI calculation selecting 2×10^6 of 2.6×10^7 determinants running on 16–64 nodes on an IBM SP3/SMP. The individual contributions are labeled as in Fig. 2.

largely attributable to its larger memory (1 GB/processor as opposed of 513 kB on the T3E). Overall these data demonstrate a sufficient scalability of the code for a large range of processors for two important massively parallel architectures available today.

III. APPLICATIONS

A. Bergman cyclization reaction

The chemistry of enediyenes has been investigated for some time because of their propensity to undergo a Bergman cyclization reaction[25,26] to paradidehydrobenzene derivatives (see figure) that are capable of lysing cellular DNA and hence cause cell death.[27] This property, if selectively activated in diseased or cancerous cells, offers the possibility of applications as cell-specific drugs against such diseases.[28] The ultimate goals is to design a compound that in cancerous cells will specifically and spontaneously undergo cyclization at physiological conditions and thus kill diseased cells. In order to predict the effectiveness of specific compounds it is important to understand the electronic structure of educt and product of the cyclization reaction as well as the height of its barrier. However, the quantum chemical description of the cyclization reaction proves difficult and interesting because of the strong change in the electronic structure of the molecule during the reaction.[28,29]

We have therefore undertaken a set of MRD-CI benchmark calculations into the Bergman cyclization of the simplest member of the enediyene family. In contrast to experimental evidence this reaction is strongly endothermic at the Hartree-Fock level of theory, which indicates that dynamic correlation effects are very important for its description. CCSD calculations,[28,29] significantly reduce deviation from experiment, but fail to account quantitatively for the ring-closure energy. Only CCSD(T) calculations, which partially account for triple excitations and thus nondynamics correlation effects, yield a quantitative agreement between experiment and theory. Taking a differential zero-point correction of $\approx$4 kcal/mol into account, this level of theory yields quantitative agreement between theory and experiment. These observations indicate that a balanced treatment of both dynamical and nondynamical correlation effects is required to quantitatively account for the reaction energetics of these compounds. Considering the N^7 scaling of the computational cost of CCSD(T), the application of this method poses significant challenges both for larger basis sets and compounds larger than the model considered here.

This investigation was motivated by two observations: An earlier MRCI (Ref. 30) study failed to reach even qualitative agreement with the experiment, presumably because the employed basis set (DZ only) was too small to account for the dynamic correlation effects. These are strongest in the educt, hence multiconfigurational MC SCF leads to a stabilization of the product with respect to the educt. Second, no calculations employing larger basis sets than DZP have been reported in the literature so far. Our goal was to establish MRD-CI as a quantitative benchmark method for the model compound at the cc-pVDZ level and to investigate larger

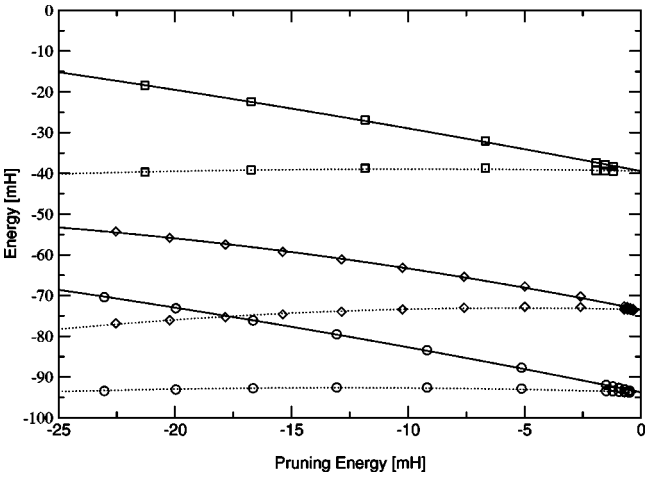

FIG. 4. Convergence of the MRD-CI energy (relative to an offset of 200 a.u.) in units of milli a.u. of the three conformations of enefiyene as a function of the selection threshold. Shown are the variational energies (solid lines) and the sum of variational and perturbative energy (dotted lines). Parallel lines permit a good extrapolation of relative energies.

basis sets with this method to ensure that the agreement obtained at that level of theory is not fortuitous.

We have performed configuration selecting MRCI calculations on product, educt, and transition state in optimized geometries[28] using cc-pVDZ, cc-pVTZ basis sets. The calculations were performed in approximate natural orbitals computed in Brillouin-Wigner multireference perturbation theory.[24]

Figure 4 shows the convergence of the variational and total energy for all three states in the cc-pVDZ basis set. The limit of zero perturbative energy corresponds to the unselected MR-SDCI calculation. The lines show the (quadratic) regression we use to extraploate to the MR-SDCI limit. For all calculations the extrapolated curves for the variational and the total energy meet in the MR-SDCI limit (to a fraction of a millihenry), which indicates the consistency and accuracy of the MRD-CI approach for this system. We note that the energies obtained for a given selection threshold result can result in rather different perturbative energies for the different isomers. Not surprisingly, the electronic structure of the transition state is most difficult to describe and yields the largest perturbative energies for a given threshold. Because second-order perturbation theory contains a systematic error in the estimation of the total energy, energies computed for a given threshold are not readily comparable.

Table I details the electronic energies of educt, transition state, and product (in a.u.) and their relative differences (in kcal/mol). For the cc-pVDZ basis these data are in good agreement with those obtained by CCSD(T) calculations. We find that differences of about 1–2 kcal/mol between the double and the triple zeta quality basis sets, in particular, for the transition state. Taking the difference in zero-point vibrational energy into account, the results are in quantitative agreement with the best available experimental data.[31,32]

B. Dinitrosoethylene

Recent investigations into the ring-opening reaction of furoxan (oxadiazole-2-oxide) into dinitrosoethylene illustrated the theoretical difficulties encountered in the elucidation the reaction mechanism. There are six possible conformers of 1,2-dinitrosoethylene, all of which might, in principle, play a role in the ring-opening reaction of furoxan, which may serve as a possible source of nitric oxide in biology. High level methods are required qualitatively account for the energetic ordering of the various conformers, in particular, the relevance of *cis-cis-trans* (cct) DNE. We follow the notation of Ref. 33 labeling the various conformers with their acronyms (c=*cis*,t=*trans*). In all there are 26 stationary points of the ground state potential energy surface of DNE.

Using configuration selecting CI we have investigated the relative energies and the singlet triplet splitting (both adiabatic and vertical) of the tct and ttt isomers in comparison with recent B3LYP, CASPT2, CASPT3, CCSD(T), and internally contracted MRCI (icMRCI) results. The geometries were optimized at the level of B3LYP discrete Fourier Transform method with an augmented $6\text{-}311++\mathrm{G}(d,p)$ basis set, for triplets the unrestricted version of this method was used. The MRCI calculations were performed in an aug-cc-pVDZ and $6\text{-}311+\mathrm{G}(2df,2pd)$ basis set in approximate natural orbitals generated in Brillouin-Wigner multireference perturbation theory.[24,34] The last basis set was used to permit a direct comparison with earlier CCSD(T) and icMRCI calculations. We used a nine orbital active space with reference selection for all calculations.

The results for the absolute energies of the conformers and electronic states are summarized in Tables II and III. Due the presence of lone pairs and strong static correlation effects, excitation energies are difficult to determine for the various conformers of DNE. For tct-DNE we find a good agreement between the Davidson corrected vertical excitation energy computed with MRD-CI and the results of icMRCI. The results for the aug-pVDZ basis and the larger $6\text{-}311++\mathrm{G}(d,p)$ are very similar, indicating convergence with respect to the basis set. There is a 3.2 kcal/mol difference to the CCSD(T) result. Similarly there is good agree-

TABLE I. Absolute (in milli a.u. relative to -230.0 H) and relative electronic energies (in kcal/mol) of the educt, transition state, and product of the ring closure reaction of enediyeneto didehydrobenzene as computed by MRD-CI and including a Davidson correction (CI+Q).

	cc-pVDZ				cc-pVTZ			
	MRD-CI	Difference	CI+Q	Difference	MRD-CI	Difference	CI+Q	Difference
Edukt	−88.9		−189.6		−262.0		−390.3	
TS	−35.0	33.8	−140.1	31.0	208.54	33.8	−342.0	30.3
Product	−73.5	9.7	−179.6	6.2	−243.8	11.7	−374.1	10.2

TABLE II. Vertical and adiabatic $S_0 \rightarrow T_1$ excitation energies of the tct-DNE (kcal/mol).

Method	Basis	Vertical	Adiabatic
DFT	6-311+G(2*df*,2*pd*)	11.6	−0.9
CCSD(T)	6-311+G(2*df*,2*pd*)	25.1	18.2
icMRCI+P	6-311+G(2*df*,2*pd*)	24.4	NA
MRD-CI+P	aug-cc-pVDZ	22.5	21.6
	aug-cc-pVTZ	22.0	21.2
	6-311+G(2*df*,2*pd*)	21.7	19.4
MRD-CI+D	aug-cc-pVDZ	23.5	23.3
	aug-cc-pVTZ	22.9	21.2
	6-311+G(2*df*,2*pd*)	23.0	19.4
MRD-CI	aug-cc-pVDZ	31.2	28.5
	aug-cc-pVTZ	30.6	27.7
	6-311+G(2*df*,2*pd*)	29.3	28.8

ment between CCSD(T) and MRD-CI+P for the adiabatic excitation energy, which has not been previously computed with icMRCI. For both vertical and adiabatic excitations energies of ttt we find good agreement between the correlated methods.

IV. SUMMARY

Benchmark methods, such as CCSD(T) or MRCI, provide useful results to our understanding of the electronic structure of molecules and of chemical reactions despite their high computational cost. It is, therefore, worthwhile to devote significant effort to the implementation of these methods on the most powerful available computational architectures, i.e., presently massively parallel machines with distributed memory. Here we reported significant improvements of our massively parallel implementation of the configuration selective MRD-CI method, which presently permits the treatment of Hilbert spaces of up to 10^{12} configurations, about 5×10^7 can be selected into the variational subspace.

TABLE III. Vertical and adiabatic $S_0 \rightarrow T_1$ excitation energies of the ttt-DNE (kcal/mol).

Method	Basis	Vertical	Adiabatic
DFT	6-311+G(2*df*,2*pd*)	15.1	−7.7
CCSD(T)	6-311+G(2*df*,2*pd*)	27.6	7.3
icMRCI+P	6-311+G(2*df*,2*pd*)	26.2	7.7
MRD-CI+P	aug-cc-pVDZ	24.9	7.8
	aug-cc-pVTZ	24.7	8.1
	6-311+G(2*df*,2*pd*)	25.2	7.4
MRD-CI	aug-cc-pVDZ	25.9	8.9
	aug-cc-pVTZ	25.9	9.0
	6-311+G(2*df*,2*pd*)	26.7	8.3
MRD-CI+D	aug-cc-pVDZ	30.6	8.0
	aug-cc-pVTZ	30.2	8.2
	6-311+G(2*df*,2*pd*)	33.4	7.4

This methodological framework permits us to perform multireference CI calculations for mid-size molecules with acceptable turnaround times. In this study we have reported benchmark accuracy results for the singlet and triplet states of various isomers of dinitrosoethylene in good agreement with other theoretical methods. We have also reported the first accurate MRCI calculations for the Bergman cyclization reaction of enediyene, which agree well with experimental data. The systematic exploration of various basis sets of different quality permits an assessment of the reliability of other calculations regarding derivative reactions.

ACKNOWLEDGMENTS

The authors gratefully acknowledge helpful discussions with G. Rauhut and N. Dobrodey. Part of this work was supported by DFG Grant No. KEI-164/11-2 and by DFG Grant No. WE 1863/10-1. The authors acknowledge the use of the supercomputer facilities at the HLRZ Karlsruhe and the NIC.

[1] B. O. Roos, Chem. Phys. Lett. **15**, 153 (1972).
[2] B. O. Roos and P. E. M. Siegbahn, in *Methods of Electronic Structure Theory*, edited by H. F. Schaefer III (Plenum, New York, 1994), p. 189.
[3] I. Shavitt, in *Modern Theoretical Chemistry*, edited by H. F. Schaefer III (Plenum, New York, 1977).
[4] S. R. Langhoff and E. R. Davidson, Int. J. Quantum Chem. **8**, 61 (1974).
[5] W. Butscher, S. Shih, R. J. Buenker, and S. D. Peyerimhoff, Chem. Phys. Lett. **52**, 457 (1977).
[6] J. Cižek, J. Chem. Phys. **45**, 4256 (1966).
[7] R. J. Bartlett and I. Shavitt, Chem. Phys. Lett. **50**, 190 (1977).
[8] R. Gdanitz and R. Ahlrichs, Chem. Phys. Lett. **143**, 413 (1988).
[9] P. Szalay and R. J. Bartlett, J. Chem. Phys. **103**, 3600 (1995).
[10] J. P. Daudey, J.-L. Heully, and J. P. Malrieu, J. Chem. Phys. **99**, 1240 (1993).
[11] R. J. Bunker and S. Peyerimhoff, Theor. Chim. Acta **12**, 183 (1968).
[12] R. J. Buenker and S. D. Peyerimhoff, Theor. Chim. Acta **35**, 33 (1974).
[13] R. J. Buenker and S. D. Peyerimhoff, Theor. Chim. Acta **39**, 217 (1975).
[14] Z. Gershgorn and I. Shavitt, Int. J. Quantum Chem. **2**, 751 (1968).
[15] B. Huron, J. Malrieu, and P. Rancurel, J. Chem. Phys. **58**, 5745 (1973).
[16] R. J. Buenker and S. D. Peyerimhoff, *New Horizons in Quantum Chemistry* (Reidel, Dordrecht, 1983).
[17] J. L. Whitten and M. Hackmeyer, J. Chem. Phys. **51**, 5584 (1969).
[18] R. J. Harrison, J. Chem. Phys. **94**, 5021 (1991).
[19] S. Krebs and R. J. Buenker, J. Chem. Phys. **103**, 5613 (1995).
[20] M. Hanrath and B. Engels, Chem. Phys. **225**, 197 (1997).
[21] F. Stephan and W. Wenzel, J. Chem. Phys. **108**, 1015 (1998).
[22] P. Stampfuß, H. Keiter, and W. Wenzel, J. Comput. Chem. **20**, 1559 (1999).
[23] P. Stampfuß and W. Wenzel, J. Mol. Struct. **506**, 99 (2000).
[24] W. Wenzel and M. M. Steiner, J. Chem. Phys. **108**, 4714 (1998).
[25] T. P. Lockhart, P. B. Commita, and R. G. Bergman, J. Am. Chem. Soc. **103**, 4082 (1981).
[26] T. P. Lockhart and R. G. Bergman, J. Am. Chem. Soc. **103**, 4092 (1981).
[27] R. Gleiter and D. Kratz, Angew. Chem. **105**, 884 (1993).
[28] E. Kraka and D. Cremer, J. Am. Chem. Soc. **122**, 8245 (2000).
[29] E. Kraka and D. Cremer, J. Am. Chem. Soc. **116**, 4929 (1994).
[30] N. Koga and K. Morokuma, J. Am. Chem. Soc. **113**, 1907 (1991).
[31] W. Roth, H. Hopf, and C. Horn, Chem. Ber. **127**, 1765 (1994).
[32] J. Gräfenstein, A. Hierpe, E. Kraka, and D. Cremer, J. Phys. Chem. **104**, 1748 (2000).
[33] M. S. J. Stevens and G. Rauhut, J. Am. Chem. Soc. **123**, 7326 (2001).
[34] W. Wenzel and K. G. Wilson, Phys. Rev. Lett. **68**, 800 (1992).